



# Validation of a Ghost Fluid Method in a Tree-Based Adaptive Volume of Fluid Solver for Two-Phase Heat and Mass Transfer

Riccardo Mereu<sup>a</sup>, Gaël Guédon<sup>a</sup>, Fabio Inzoli<sup>a</sup>, Emanuela Colombo<sup>a</sup> and Jacopo Buongiorno<sup>b</sup>

<sup>a</sup> Politecnico di Milano, Dipartimento di Energia, Via Lambruschini, 4, 20156 Milano, Italy  
<sup>b</sup> Massachusetts Institute of Technology, 77 Massachusetts Ave., Room 24-206, Cambridge, MA 02139, USA  
E-mail: riccardo.mereu@polimi.it

## Description of the problem

Multiphase flows involving gas bubbles in liquid are present in many industrial applications, e.g. chemical reactors, oil & gas processes, cooling of nuclear reactors and fossil fuel boilers. The complex phenomena related with these applications have been recently studied via Computational Fluid Dynamics (CFD). Usually, simplified configurations are studied in order to investigate separately the effects of the different governing phenomena. Various models were proposed in the last decade to simulate boiling phenomena with and without the interaction with solid surfaces. Models based on Volume of Fluid (VOF), Level Set (LS), Coupled Level Set Volume of Fluid (CLSVOF), and Front Tracking methods were proposed and validated by using typical test-cases such as inviscid and viscous static bubble surrounded from a stagnant fluid, isothermal rising bubble in a stagnant fluid, etc. Models used to simulate boiling phenomena have to include ad-hoc methods for the calculation of the interface curvature, the discretization of pressure jump due to surface tension, the discretization of velocity jump due to mass transfer, the discretization of temperature with reference to the problem of Dirichlet boundary conditions at the interface, and the computation of jump in temperature gradient (mass transfer flux calculation). The capabilities of the VOF-YOUNGS, CLSVOF, VOF-HF (Popinet, 2003) methods for the calculation of interface curvature, as well as the Continuum Surface Force and Ghost Fluid Method for discretization of pressure jump are here analyzed.

## Test-case

The test-case reproduces the scenario of a gas bubble rising under the effect of buoyant forces in stagnant liquid reproducing some of the many physical conditions reported in the map proposed by Clift et al. (1978). Fluids are initially at rest, gravity is the only body-force acting and the bubble topology is strongly time dependent. After the initial transient the velocity of the rising bubble reaches an asymptotic value defined as terminal velocity. Many different sizes and shapes of bubbles observed at different regimes are defined by using three dimensionless groups, Reynolds (Re), Morton (Mo) and Eotvos (Eo) (or Bond) numbers. In the Table below the fluid properties are reported along with the characteristic size of the bubble for three different scenarios. The choice of the initial diameter range over three orders of magnitude from  $\mu\text{m}$  to  $\text{cm}$  is motivated by the typical sizes of the water bubble in nucleate boiling (from a few  $\mu\text{m}$  to  $\text{mm}$ ) and the typical size used for the test-case of rising bubble ( $\text{cm}$ ). For the 'Medium' and 'Small' cases, the liquid water and air properties are used, thus maintaining a constant Mo. For the 'Large' scenario with a larger diameter the viscosity ratio was modified in order to obtain a value of 100 and obtaining Re numbers lower than the transition value.

	$d_e$ [m]	$\rho_l$ [kg/m <sup>3</sup> ]	$\rho_g$ [kg/m <sup>3</sup> ]	$\rho_l/\rho_g$ [-]	$\mu_l$ [kg/ms]	$\mu_g$ [kg/ms]	$\mu_l/\mu_g$ [-]	$\sigma$ [N/m]	$U$ [m/s]	Mo (logMo)	Eo	Re
Large - cm	0.025	1000	1.225	816	0.075	$7.5 \cdot 10^{-4}$	100	0.0728	0.285	$8.0 \cdot 10^{-4}$ (-3.1)	84.22	95
Medium - mm	0.0009	1000	1.225	816	0.001	$1.73 \cdot 10^{-5}$	58	0.0728	0.14	$2.54 \cdot 10^{-11}$ (-10.6)	0.109	126
Small - $\mu\text{m}$	0.0003	1000	1.225	816	0.001	$1.73 \cdot 10^{-5}$	58	0.0728	0.028	$2.54 \cdot 10^{-11}$ (-10.6)	0.012	8

## Numerical method

Commercial ANSYS-Fluent and open-source Gerris (Popinet, 2003) codes are used for this test-case in order to compare different methods for reconstruction of the interface and of its curvature. In the former the VOF-YOUNGS and CLSVOF methods are available, while in the latter a VOF-HF method is used in the standard code and in the modified version with the Ghost Fluid Method proposed in Guédon et al. (2012). Both codes are able to work with a 2D-axisymmetric domain coupled with a multiphase solver. The sizes of the domain are defined using the initial diameter of the bubble  $d_e$  as characteristic length. A bubble of diameter  $d_e$  is centered at  $(2d_e, 0)$  in  $x$  and  $y$  direction, respectively, in a 2D-axisymmetric rectangular domain where the axis  $y=0$  represents the revolution axis.

The numerical modeling is based on the Navier-Stokes equations in both phases and an interface transport equation for VOF or LS depending on the model used. A constant surface tension coefficient is imposed and no phase-change takes place at the interface. Additional grids have been used with local and dynamic refinements to obtain a sensitivity analysis of the grid.

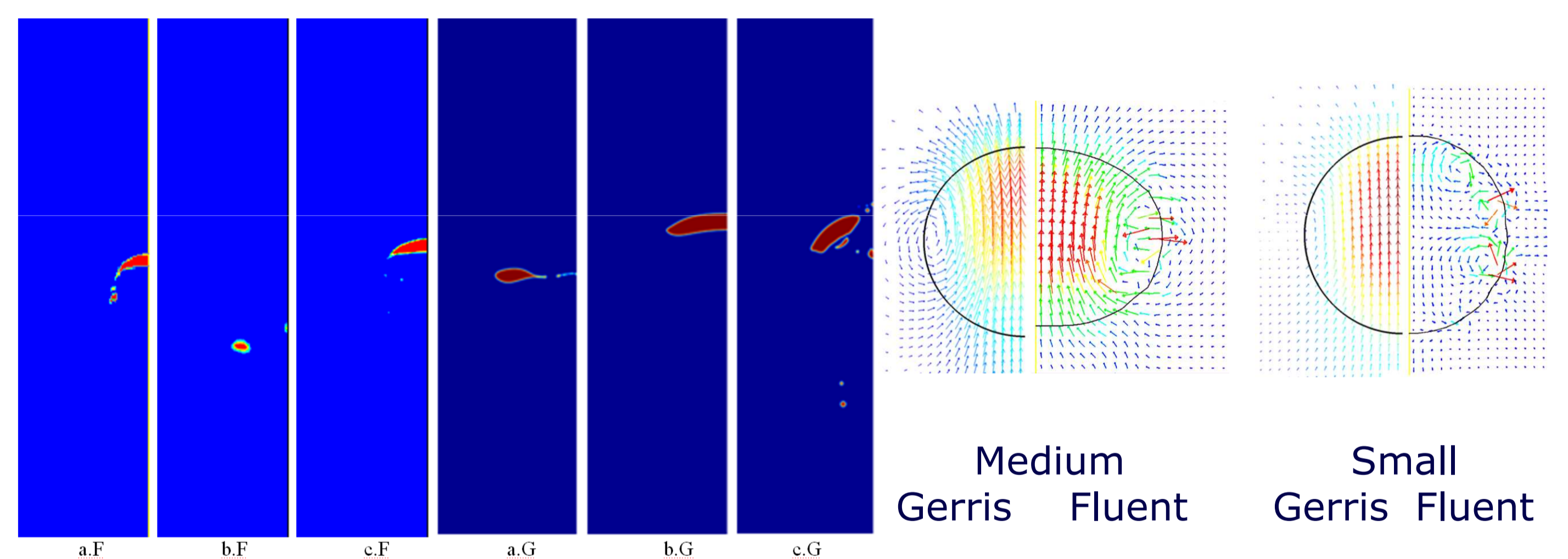
	Method	
	Fluent	Gerris
Pressure-Velocity coupling	PISO - non iterative	Projection method
Temporal term	First order (Euler implicit)	Second order (Godunov) or First order
Spatial term: gradient	Least Squares Cell based	Second order
Spatial term: pressure	PRESTO!	Second order
Spatial term: momentum	Third order	Second order
Interface reconstruction	PLIC	PLIC

Same boundary conditions are imposed for both codes. A constant value for the pressure is applied to the upper boundary of the rectangular domain, axisymmetric conditions to the right boundary, and symmetric conditions (no gradient normal to the boundary are permitted) to left and bottom boundaries. Table above shows the method used for discretization of the governing equations.

## Results

All the simulations are carried out with two different grid sizes: a 'uniform' grid, and an 'adapted' grid with local dynamic refinement allowing for 1 (ANSYS-Fluent) and 2 (Gerris) additional levels of refinement around the interface. The results obtained with the selected domains and for both 'uniform' and 'adapted' grids are reported in the Table below for ANSYS-Fluent VOF-YOUNGS (Fluent VOF) and CLSVOF (Fluent CLSVOF) methods and for the original version of the Gerris code (Gerris original), an original version with a 1st order scheme for the temporal discretization (Gerris 1st order), and the version with 1st order scheme for the temporal discretization and a Ghost Fluid Method (Gerris GFM). For the 'Large' case an expected skirted - spherical-cap shape is observed with all methods, while the break-up of the bubble is observed in all cases with uniform (coarser) grid. The complete destruction of the bubble for the Fluent CLSVOF case (b.F), for which no terminal velocity values can be obtained, is also observed.

Case	Grid	Terminal Velocity U [cm/s] (error $ U_{exp}-U_{num} /U_{exp} \cdot 100$ [%])					
		Clift et al., 1978	Fluent VOF	Fluent CLSVOF	Gerris original	Gerris 1 <sup>st</sup> order	Gerris GFM
Large - cm	uniform	28.5	28.2 (1.1)	Not Converged	31.9 (11.9)	18.9 (33.7)	29.9 (4.9)
	break-up		yes	yes	yes	yes	yes
	adapted		27.9 (2.1)	27.8 (2.5)	28.0 (1.8)	31.9 (11.9)	31.9 (11.9)
	break-up		no	no	yes	no	yes
Medium - mm	uniform	14	19.0 (35.7)	23.5 (67.9)	21.9 (56.4)	20.2 (44.3)	11.2 (20)
	adapted		18.8 (34.3)	23.0 (64.3)	21.3 (52.14)	22.5 (60.7)	19.3 (37.9)
Small - $\mu\text{m}$	uniform	2.8	Not Converged	Not Converged	5.0 (78.6)	4.4 (57.1)	4.8 (71.4)
	adapted		5.0 (78.6)	Not Converged	4.3 (53.6)	4.2 (50)	4.3 (53.6)



Images of bubble for 'Large' case of Fluent-VOF-uniform (a.F), Fluent-CLSVOF-Images (b.F), Fluent-VOF-adapted (c.F), Gerris-original-adapted (a.G), Gerris-1storder-adapted (b.G), and Gerris-GFM-adapted (c.G). The Fluent cases are at  $t=0.39\text{s}$  (a.F, c.F) and  $t=0.307\text{s}$  (b.F), Gerris cases are at  $t=1.11\text{s}$  (a.G, b.G) and  $t=0.39\text{s}$  (c.G) are reported in the Figure above (left).

For both 'Medium' and 'Small' cases an expected spherical shape is observed without any break-up. For the 'Medium' case all the methods are able to reproduce the rising bubble with small improvements when the adapted grid is used in ANSYS-Fluent cases. The regular spherical shape is well reproduced by Gerris without any deformation of the bubble, while in ANSYS-Fluent cases an unstable behavior is observed with unphysical peaks of velocity inside the bubble (Figure above, middle). This behavior in the 'Medium' case only slightly influences the rising velocity of the bubble, while the influence is more evident in the 'Small' case (Figure above, right) where the rising velocity is regular only for VOF adapted case. For other cases (CLSVOF uniform and adapted, and VOF uniform) a smooth rising velocity is not observed. The difference between two methods is evident in the upper part of the bubble (Figure above middle and right), where in ANSYS-Fluent the vortex is not physical and the high velocities deform the bubble, while in Gerris a physical vortex is observed, maintaining a spherical shape.

## Conclusions

In the 'Large' case similar behavior between tested methods is observed with some limitations in reproducing the correct shape of the bubble with relatively coarse grid especially for the Fluent CLSVOF. 'Medium' and 'Small' cases show large errors in the rising bubble velocity predictions, highlighting the limits of the curvature reconstruction methods used in the ANSYS-Fluent code. The presence of spurious currents around the interface becomes important for smaller bubbles and the rising velocity seems to be strongly affected by such currents. This behavior is not observed in the Gerris simulations, where a circular bubble with a terminal asymptotic velocity and a physical velocity field around and inside the bubble are reproduced.

## References

- Clift, Grace, Weber (1978). Academic Press, Inc., New York.  
Guédon, Mereu, Inzoli, Colombo, Buongiorno (2012). ECI 8th, 3-7 June 2012, Lausanne, Switzerland.  
Popinet (2003). Journal of Computational Physics, Vol. 190, pp. 572-600.